JOURNAL OF SOLID STATE CHEMISTRY 63, 290–294 (1986)

Metal–Insulator Transition in the System $(Ca_{1-x}La_x)MnO_{2.97}$ $(0.05 \leqq x \leqq 0.4)$

H. TAGUCHI[1]

Osaka Prefectural Industrial Research Institute, Nishi-Ku, Osaka 550, Japan

AND M. SHIMADA

Department of Applied Chemistry, Faculty of Engineering, Tohoku University, Sendai 980, Japan

Received August 26, 1985; in revised form November 25, 1985

The electrical resistivity of $(Ca_{1-x}La_x)MnO_{2.97}$ $(0.05 \leqq x \leqq 0.4)$ was measured in the temperature range from 80 to 1000 K. All manganates are *n*-type semiconductors below room temperature. Below 125 K, the electrical resistivity follows the Mott's $T^{-1/4}$ law indicating the possible occurrence of variable hopping of electrons due to Anderson localization. Above ca. 400–450 K, all manganates exhibit a metal–insulator transition without crystallographic change. From the results of magnetic measurement, the mechanism of the metal–insulator transition is explained by the band model of covalency criterion for localized vs collective electrons in oxides with the perovskite structure.

Introduction

$CaMnO_3$ has an orthorhombic perovskite-type structure and exhibits a weak ferromagnetism with $T_N = 123$ K (*1*). Wollan and Koehler synthesized the non-stoichiometric $CaMnO_{3-\delta}$, and examined its crystallographic and magnetic properties (*2*). The cell constants of $CaMnO_{3-\delta}$ were independent of the oxygen content, but Néel temperatures (T_N) increased with decreasing the oxygen content. Taguchi reported that $CaMnO_{3-\delta}$ were *n*-type semiconductors, and log ρ (ρ: electrical resistivity) vs $T^{-1/4}$ was linear and log ρ decreased with decreasing the oxygen content below 360 K (*3*). The electrical properties of $CaMnO_{3-\delta}$ were explained by the variable range hopping of electrons (*4*, *5*).

Many investigations on the substitution of La^{3+} ion by Ca^{2+}, Sr^{2+} and Ba^{2+} ions in $LaMnO_3$ have been reported (*6*, *7*). Jonker and Van Santen first reported that $(La_{1-x}Ca_x)MnO_3$ was ferromagnetic in the range $0.1 \leqq x \leqq 0.5$ (*6*). Wollan and Koehler reported that the ferromagnetic and antiferromagnetic properties of $(La_{1-x}Ca_x)MnO_3$ strongly depend on its chemical composition (*2*). $(La_{0.65}Ca_{0.35})MnO_3$ was ferromagnetic, but above and below $x = 0.35$ $(La_{1-x}Ca_x)MnO_3$ was antiferromagnetic.

$LaMnO_3$ is a semiconductor with an electrical resistivity of 10^5 Ω cm at 200 K (*8*). The electrical resistivity of $(La_{1-x}Ca_x)MnO_3$ decreased with increasing x in the range $0 \leqq x \leqq 0.2$. In the range $0.3 \leqq x \leqq 0.5$,

[1] To whom all correspondence should be addressed.

0022-4596/86 $3.00

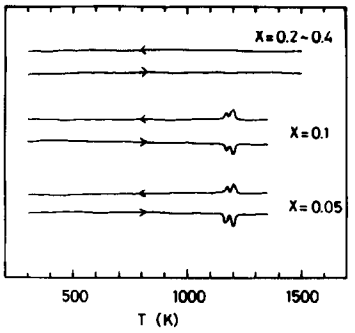

FIG. 1. DTA curve in the system $(Ca_{1-x}La_x)MnO_{2.97}$.

$(La_{1-x}Ca_x)MnO_3$ was metallic at low temperature, and exhibited a metal–semiconductor transition near the Curie temperature (*9*). According to Tanaka *et al.*, the metal–semiconductor transition of $(La_{0.8}Ca_{0.2})MnO_3$ was explained by the localization of the hole forming the magnetic spin molecule for Mn^{3+} ion in its neighbor (*10*).

In the present study, an attempt was made to synthesize the perovskite-type $(Ca_{1-x}La_x)MnO_{2.97}$ $(0.05 \leqq x \leqq 0.4)$ in order to study its electrical properties from the results of both electrical resistivity and the magnetic susceptibility measurements. These results will provide some information for discussing the behavior of 3*d* electrons of Mn ions in the perovskite oxide system.

Experimental

All $(Ca_{1-x}La_x)MnO_3$ $(0.05 \leqq x \leqq 0.4)$ samples were prepared using a standard ceramic technique. Powders of La_2O_3, $CaCO_3$, and $MnCO_3$ were weighed in the desired proportions and milled for a few hours with acetone. After the mixed powders were dried at 100°C, they were calcined in air at 800°C, then fired at 1300°C for 24 hr in a flow of pure oxygen gas. For measuring the resistivity, the powder was compressed into a pellet form under a pressure of 50 MPa, and then the pellet was sintered at 1300°C for 12 hr in a flow of pure oxygen gas. The oxygen deficient materials obtained in this way were annealed at 600–700°C in air for 50 hr.

The phases of the samples were identified by X-ray powder diffraction with filtered Cu$K\alpha$ radiation. The oxygen content in each samples was determined by the oxidation–reduction method (*11*). The electrical resistivity was measured by a standard four-electrode technique in the temperature range from 80 to 1000 K. Magnetic susceptibility was measured by a magnetic torsion balance in the temperature range from 300 to 700 K. Phase transition of the sample was measured by differential thermal analysis (DTA) in the temperature range from 300 to 1523 K.

Results and Discussion

The oxygen content of all samples $(Ca_{1-x}La_x)MnO_{3-\delta}$ $(0.05 \leqq x \leqq 0.4)$ annealed at 600–700°C in air was determined to be 2.97 ($\delta = 0.03$) from chemical analysis. X-Ray powder diffraction patterns of $(Ca_{1-x}La_x)MnO_{2.97}$ were completely indexed as the pervoskite-type structure. Figure 1 shows the results of differential thermal analysis (DTA) of $(Ca_{1-x}La_x)MnO_{2.97}$. $(Ca_{1-x}La_x)MnO_{2.97}$ $(0.05 \leqq x \leqq 0.2)$ gave exthothermic peaks at ca. 1160–1190 K. On the other hand, $(Ca_{1-x}La_x)MnO_{2.97}$ $(0.2 \leqq x \leqq 0.4)$ did not give either exothermic or endothermic peak up to 1523 K. These results indicate that the crystal structure of $(Ca_{1-x}La_x)MnO_{2.97}$ $(0.05 \leqq x \leqq 0.4)$ did not change below 1160 K.

The electrical resistivity data in the temperature range from 80 to 1000 K is shown in Fig. 2. Below room temperature, all samples were *n*-type semiconductors and the electrical resistivity (ρ) increased with increasing x. The activation energy calculated from the linear portion of $\log \rho$ vs $1/T$ increased monotonically with increasing x as shown in Table I. Below 125 K, $\log \rho$ vs

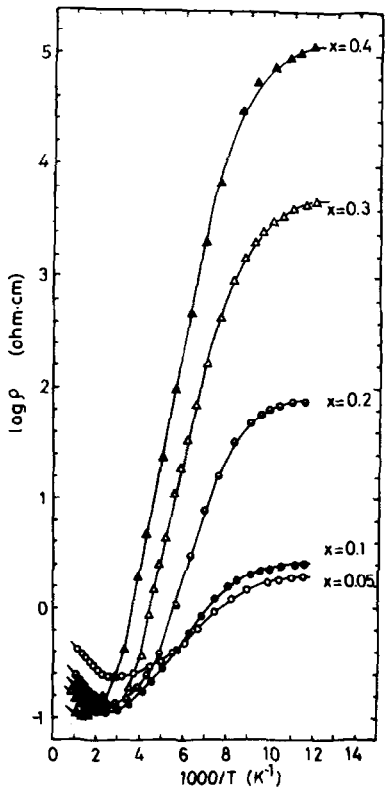

FIG. 2. Electrical resistivity vs $1/T$ in the system $(Ca_{1-x}La_x)MnO_{2.97}$.

$1/T$ was nonlinear. The relation between log ρ vs $T^{-1/4}$ for $0.05 \leqq x \leqq 0.4$ samples is shown in Fig. 3. As seen in Fig. 3 log ρ vs $T^{-1/4}$ was

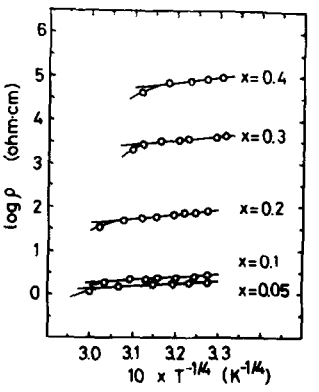

FIG. 3. Electrical resistivity vs $T^{-1/4}$ in the system $(Ca_{1-x}La_x)MnO_{2.97}$.

linear below ca. 100 K and log ρ strongly depended on the chemical composition. From these results, the electrical properties of $(Ca_{1-x}La_x)MnO_{2.97}$ was explained by the variable range hopping of electrons by analogy with $CaMnO_{3-\delta}$ at low temperature (*3–5*). Above ca. 400–450 K, $(Ca_{1-x}La_x)MnO_{2.97}$ had a metallic temperature coefficient and the electrical resistivity increasing temperature as seen in Fig. 2. From the result of DTA shown in Fig. 1, it is said that the metal–insulator transition in $(Ca_{1-x}La_x)MnO_{2.97}$ occurred without the phase transition.

Wollan and Koehler reported that

TABLE I

THE ACTIVATION ENERGY (E), PARAMAGNETIC CURIE TEMPERATURE (T_θ) AND EFFECTIVE MAGNETIC MOMENT (μ_{eff}) IN THE SYSTEM $(Ca_{1-x}La_x)MnO_{2.97}$

		$300 \leqq T \leqq 450$–500		450–$500 \leqq T \leqq 700$	
x	E (eV)	T_θ (K)	μ_{eff}	T_θ (K)	μ_{eff}
0.05	0.04	—	—	—	—
0.1	0.05	150	2.96	56	3.35
0.2	0.12	—	—	—	—
0.3	0.18	218	3.34	203	3.50
0.4	0.19	—	—	—	—

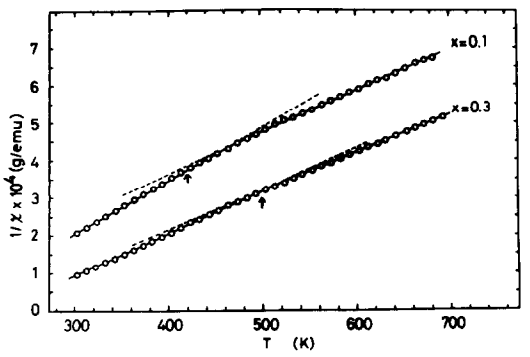

FIG. 4. Inverse magnetic susceptibility vs temperature in the system $(Ca_{1-x}La_x)MnO_{2.97}$.

$(La_{1-x}Ca_x)MnO_{3-\delta}$ was antiferromagnetic in the range $0.6 \leqq x \leqq 1.0$, and the Néel temperature (T_N) increased with decreasing x (*2*). The temperature dependence of the inverse susceptibility ($1/\chi_g$) of $(Ca_{1-x}La_x)MnO_{2.97}$ ($x = 0.3$ and 0.4) is shown in Fig. 4. The $1/\chi_g$–T curve obeyed the Curie–Weiss law, and had a deflection point at ca. 450–500 K. In Fig. 4, the arrows indicate the metal–insulator transition of each sample. The paramagnetic Curie temperature (T_θ) and the effective magnetic moment (μ_{eff}) calculated from the linear portions below and above 450–500 K in the $1/\chi_g$–T curve are listed in Table I. T_θ decreased and μ_{eff} increased above ca. 450–500 K. These results suggested that the change of the electron configuration of Mn ions in $(Ca_{1-x}La_x)MnO_{2.97}$ occurred above 450–500 K, and affected the electrical conductivity.

Goodenough proposed an energy band scheme consisting of the partially filled σ^* orbitals and π^* hole, and the band scheme for the perovskite structure (*12*). The localized π^* orbitals of α and β spin at a given cation are split by the intraatomic exchange (E_{ex}), and collective σ^* orbitals were also splite by E_{ex}. The magnitude of the electrostatic field (Δ) depends on both particular anion complex and valency state of cation. μ_{eff} of $(Ca_{1-x}La_x)MnO_{2.97}$ increases above 450–500 K as shown in Table I. The Mn^{4+} ion ($3d^3$) had the electron configuration of $(d\varepsilon)^3(d\gamma)^0$. On the other hand, Mn^{3+} ion with $3d^4$ electron configuration have both low- and high-spin state with the $(d\varepsilon)^4(d\gamma)^0$ and $(d\varepsilon)^3(d\gamma)^1$, respectively. The calculated value of μ_{eff} for $(Ca_{0.9}La_{0.1})MnO_{2.97}$ with the low-spin state of Mn^{3+} ion and the high-spin state of Mn^{3+} ion is 3.71 and 4.04 μ_B, respectively. Although the observed value of μ_{eff} listed in Table I is smaller than that calculated, it is consider that the spin state of Mn^{3+} ion changed from low ($E_{ex} < \Delta$) to high ($E_{ex} < \Delta$) above T_t (metal–insulator transition point). Below T_t, the electrons existed in the localized π^* orbital of α and β spins. Above T_t, the collective σ^* orbital of α spin overlapped with the localized π^* orbital of β spin. Since the electrons partially filled both collective σ^* and localized π^* orbitals, $(Ca_{1-x}La_x)MnO_{2.97}$ exhibited metallic behavior at high temperature.

It is concluded that $(Ca_{1-x}La_x)MnO_{2.97}$ ($0.05 \leqq x \leqq 0.4$) exhibits a metal–insulator transition without the phase transformation at high temperature. Both T_θ and μ_{eff} of $(Ca_{1-x}La_x)MnO_{2.97}$ changed above 400–450 K, and the electrical properties were strongly influenced by the magnetic properties. The mechanism of the metal–insulator transition in $(Ca_{1-x}La_x)MnO_{2.97}$ is explained by the band model proposed by Goodenough (*12*).

References

1. J. B. MACCHESNEY, H. J. WILLIAMS, J. F. POTTER, AND R. C. SHERWOOD, *Phys. Rev.* **164,** 779 (1967).
2. E. O. WOLLAN AND W. C. KOEHLER, *Phys. Rev.* **100,** 545 (1955).
3. H. TAGUCHI, *Phys. Status Solidi A* **88,** K79 (1985).
4. V. JOSHI, O. PARKASH, G. N. RAO, AND C. N. R. RAO, *J. Chem. Soc., Faraday Trans. 2,* 75 (1979).
5. N. F. MOTT, *Adv. Phys.* **21,** 785 (1972).
6. G. H. JONKER AND J. H. VAN SANTEN, *Physica* **16,** 337 (1950).

7. G. H. JONKER, *Physica* **22,** 707 (1956).
8. G. MATSUMOTO, "Ferrites: Proc. International Conf., July 1970, Japan," p. 578.
9. J. H. VAN SANTEN AND G. H. JONKER, *Physica* **16,** 599 (1950).
10. J. TANAKA, M. UMEHARA, S. TAMURA, M. TSUKIOKA, AND S. EHARA, *J. Phys. Soc. Japan* **51,** 1236 (1982).
11. B. E. GUSHEE, L. KATZ, AND R. WARD, *J. Amer. Chem. Soc.* **79,** 5601 (1957).
12. J. B. GOODENOUGH, *J. Appl. Phys.* **37,** 1415 (1966).